INFECTION AND IMMUNITY, Mar. 1981, p. 1214-1222
0019-9567/81/031214-09$02.00

Vol. 31, No. 3

Enhancement of Plaque Formation and Cell Fusion of an Enteropathogenic Coronavirus by Trypsin Treatment

J. STORZ,[1]* R. ROTT,[2] AND G. KALUZA[2]

Department of Microbiology, Colorado State University, Fort Collins, Colorado 80523,[1] and Virology Institute, Justus Liebig University, Giessen, West Germany[2]

Plaque formation, replication, and related cytopathic functions of the enteropathogenic bovine coronavirus strain L9 in bovine fetal thyroid (BFTy) and bovine fetal brain (BFB) cells were investigated in the presence and absence of trypsin. Plaque formation was enhanced in both cell types. Plaques reached a size with an average diameter of 5 mm within 4 days with trypsin in the overlay, whereas their diameter remained less than 1 mm at this time after plating without trypsin in the overlay. Fusion of both cell types was observed 12 to 18 h after infection when trypsin was present in the medium. Fusion was not observed in infected BFB cell cultures and was rarely observed 48 h after infection of BFTy cells maintained with the trypsin-free medium. The largest polycaryons formed had 15 to 22 nuclei. They then lysed and detached. Cell fusion depended on de novo synthesis of hemagglutinin and infectivity. Fusion from without was not observed. Virus produced under trypsin-enhancing conditions accompanied by cell fusion did not lyse mouse erythrocytes that reacted with L9 coronavirus hemagglutinin. Trypsin-treated, infected BFTy cultures produced coronaviral particles that excluded stain from the envelope confinement. These virions had uniformly shorter surface projections than did the viral forms generated by trypsin-free cell cultures.

Coronaviruses are important causes of upper respiratory illness, encephalitis, hepatitis, or enteric disease of humans or animals (14). Some enteropathogenic coronavirus strains have been adapted, with difficulty, to multiply in cultured cells (13, 16, 20, 22, 27), and others replicate only in organ cultures (3, 4, 14). Cultivation remained unsuccessful in numerous instances in which electron microscopic examination revealed the presence of coronavirus infection (5, 7, 12, 21). This property characterized particularly the strains causing intestinal infection. Many enteropathogenic coronavirus strains were maintained by inoculating the respective original hosts (5, 7, 12, 21). Some coronavirus strains were adapted to specific cell lines, in which they induced various cytopathic changes and occasionally polycaryocytosis (13, 20, 27, 28). Defining methods for accurate quantitation of infectivity by plaque assays succeeded with just a few coronavirus-cell culture systems (14, 20, 27, 28). We explored conditions for cultivating an enteropathogenic coronavirus strain in primary and low-passage bovine fetal thyroid (BFTy) and bovine fetal brain (BFB) cells. The enteropathogenic bovine coronavirus strain L9 multiplied in these cells with cytopathic effects as well as with cell fusion and plaque formation, which depended on the presence of trypsin in the medium. The evidence for these findings is presented in this report.

MATERIALS AND METHODS

Virus strain. The enteropathogenic bovine coronavirus strain L9 was used. It had been passaged 42 times in bovine fetal kidney (BFK) cells with mildly cytopathic changes after original isolation by Mebus et al. from diarrhea fluid of a calf with enteritis (16, 22).

Cells. BFTy cells were dispersed and cultured from the thyroid gland of an 8-month-old bovine fetus by methods previously described (23). Fibroblast-like BFB cells were cultured from brains of 2- to 4-month-old bovine fetuses. The brain tissue was not trypsinized; instead, it was aspirated with a syringe and then homogenized by repeated passage through an 18-gauge needle fitted to a syringe. The cells were cultured in Eagle minimum essential medium (MEM) or its Dulbecco modification (MEMD), with 100 U of penicillin, 100 μg of streptomycin, and 50 μg of gentamicin per ml. Heat-inactivated bovine fetal calf or lamb serum was added at 10% to the growth medium. The serum was tested previously in the microimmunodiffusion test for antibodies against the bovine coronavirus strain L9 (24).

Propagation and growth curve of L9 coronavirus strain with and without trypsin. L9 virus was adapted to and propagated in BFTy and BFB cells incubated at 37°C in a CO_2 incubator. Cell monolayers in 25-ml plastic culture flasks were washed twice

with serum-free medium, and the viral inoculum was allowed to adsorb for 1 h. Paired, inoculated cell monolayers were washed and given serum-free medium or such medium with 10 μg of trypsin (Difco Laboratories, Detroit, Mich.; 1:250) per ml. This concentration of trypsin did not affect the monolayers of the two cell types used, but concentrations of 15, 20, 25, and 30 μg per ml caused increasing cell retraction, rounding, and detachment.

To establish the growth pattern of L9 in BFTy cells, they were grown in 25-ml plastic culture flasks. The monolayered cells were washed, inoculated with 1 ml of BFTy-propagated virus with an infectivity of 4×10^6 plaque-forming units. Adsorption at 37°C for 1 h was followed by three washes with serum-free medium. Paired sets of infected BFTy cultures were then given MEM or MEM plus 10 μg of trypsin per ml. Immediately after adsorption and at intervals of 3, 6, 12, 18, 24, 30, 36, 48, and 60 h later, the medium of pairs of infected BFTy cultures was decanted and centrifuged separately at 2,000 rpm for 10 min to settle cellular material. The supernatant fluid was assayed for cell-released hemagglutinin (HA) and plaque-forming unit infectivity. The sediment of the medium centrifugation was suspended in 1 ml of fresh medium, which was then added to the cells in the respective culture flasks, which were frozen and thawed to remove the cells. These cell suspensions were sonicated before being assayed for cell-associated HA and plaque-forming units.

Cytological evaluation of trypsin action on L9 cytopathic effect. BFTy and BFB cells were grown on 35-mm plastic petri dishes. When complete monolayers had formed, the cells were infected with L9 virus that had been propagated in the respective cell type. The 1-ml inoculum had an infectivity of 2×10^6 to 4×10^6 plaque-forming units. After adsorption for 1 h, serum-free medium was added to one half of the sets of cultures, and the same medium containing 10 μg of trypsin per ml was added to the other half. Paired infected cultures with and without trypsin were withdrawn after virus adsorption and 3, 6, 12, 18, 20, 24, 30, 36, and 48 h later. A set of uninoculated cell cultures was treated identically and collected during late sampling periods. The cultures were washed, fixed in Bouin solution, and further processed for staining by the Giemsa method. Cover slips were mounted with Epon 812 into the middle of each culture dish for microscopic evaluation and for photography with a Leitz Orthomat microscope.

Plaque assay. Conditions for plaque assay of L9 infectivity were explored with BFTy and BFB cells. They were grown in 60-mm plastic petri dishes, as described above. The inoculum per plate was 0.25 ml of the various virus dilutions, which adsorbed for 1 h at 37°C. The inoculum fluid was then withdrawn, and 5 ml of overlay medium was added. Three overlay combinations were tested with MEMD: 0.6% agarose, 0.9% Noble agar, and 1% sodium carboxymethyl cellulose. These combinations of overlay media were used serum free or with 3% bovine fetal calf serum. Ultimately, only overlay medium with 0.6% agarose and serum-free MEMD was employed. The effect of 10 μg of trypsin per ml of overlay on plaque size, morphology, and time of appearance was also tested. At different daily intervals after plating, plaque plates were stained with 0.02% neutral red in saline and fixed with a 4% Formalin saline solution for plaque measurements and photography.

Hemagglutination and hemolysis tests. The microtiter method was used to detect L9 coronavirus HA for washed mouse erythrocytes as a 0.2% suspension in pH 7.2- phosphate-buffered saline. The agglutination reaction occurred at room temperature for 2 h or overnight under 8°C refrigeration.

Coronavirus propagated in BFTy and BFB cells in the presence or absence of trypsin was also tested for mouse erythrocyte hemolytic activity. Various virus samples were mixed in 0.25-ml amounts with 0.5 ml of 2% mouse erythrocytes in phosphate-buffered saline. The mixture was incubated at 37°C for 1 h and centrifuged at 2,000 rpm for 10 min; then, absorbance of the supernatant was measured in a dual-beam Beckman model 25 spectrophotometer at 415, 540, and 555 nm. Supernatant fluid from controls of completely lysed or intact mouse erythrocytes were included to compare the degree of hemolysis.

Virus confirmation. L9 coronavirus propagated under different conditions was analyzed morphologically by electron microscopic examination. Medium from infected cell cultures was centrifuged at 12,000 rpm for 20 min. A drop of the supernatant fluid was deposited on gel consisting of 0.4% agarose and 0.4% agar in barbital buffer of pH 8.2. Formvar carbon-coated grids were placed onto the specimen drops on the gel surface for 5 min to load the grids. The grids were then stained negatively with 2% phosphotungstic acid and examined with an HU-12 Hitachi electron microscope.

RESULTS

Effect of trypsin on plaque induction. An overlay of sodium carboxymethyl cellulose or Noble agar in combination with MEMD, MEM, Lavit, or 199 media with and without 3% inactivated bovine fetal calf serum did not lead to plaque formation in BFTy and BFB cells during a 7-day observation period. Agarose with MEMD and MEM, but not 199 or Lavit medium, facilitated plaques in both cell types. They were first detected 4 days after incubation, reached a measurable size of 1.1 mm in diameter on day 5, and enlarged slightly during the following days (Table 1). They had turbid centers and fuzzy margins (Fig. 1a). Serum in the overlay had no modulating effect. A striking enhancement of plaque formation was observed when 10 μg of trypsin per ml was present in the agarose-MEM or -MEMD overlays. At 3 days after plating, large, clear, round plaques with sharp edges were present (Fig. 1b and 2). The size was further enlarged to a diameter of 5 mm on day 4 (Table 1). When virus was pretreated with trypsin or trypsin was present only during viral adsorption, plaque enhancement was not observed. The plaque numbers observed with and

TABLE 1. *Comparison of conditions for plaque formation by bovine coronavirus strain L9 in BFTy and BFB cells*

Overlay	Cell type	Plaque size (mm) on days after plating:				
		3	4	5	6	7
Carboxymethyl cellulose plus MEMD	BFTy	—[a]	—	—	—	—
	BFB	—	—	—	—	—
Noble agar plus MEMD	BFTy	—	—	—	—	—
	BFB	—	—	—	—	—
Agarose plus MEMD	BFTy	—	±(<1.0)	+(1.1)[b]	+(1.3)	ND[c]
	BFB	—	±(<1.0)	+(1.1)	+(1.4)	ND
Agarose plus MEMD plus trypsin	BFTy	+(3.8)[b]	+(5.0)	+(5.0)	ND	ND
	BFB	+(4.1)	+(5.0)	+(5.6)	ND	ND

[a] —, No plaques detectable.
[b] Plaques present. Average diameter of 7 to 12 plaques per plate.
[c] ND, Not done.

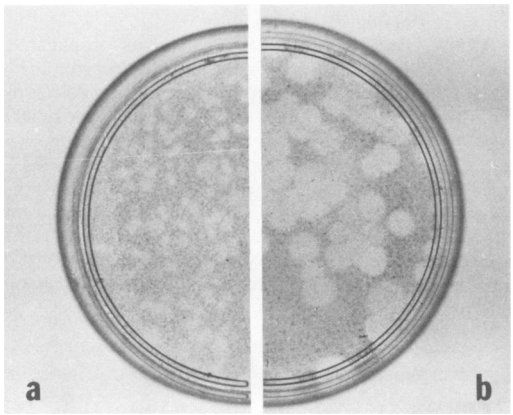

FIG. 1. *Plaques induced by enteropathogenic coronavirus strain L9 in BFTy cells 6 days (a) after plating without trypsin and 4 days (b) after plating with 10 μg of trypsin per ml of overlay.*

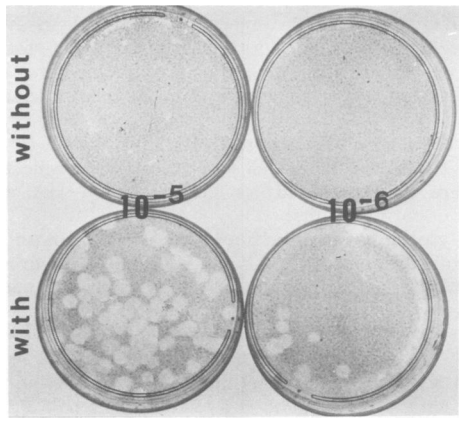

FIG. 2. *Comparison of plaque formation 3 days after plating without and with trypsin in the overlay. Plates were reduced to half their size.*

without trypsin depended linearly on the virus dilutions plated (Fig. 2).

Modulation of cytopathic changes and cell fusion by trypsin. Replication of L9 coronavirus in BFTy and BFB cells caused progressive cytopathic changes (Fig. 3 and 4). Few small polycaryons were observed 45 h after infection of BFTy cells (Fig. 3g), and none was observed in infected BFB cell cultures free of trypsin.

The presence of 10 μg of trypsin per ml in the medium enhanced the cytopathic changes and modulated viral cytopathic functions to induce numerous polycaryons in BFTy as well as in BFB cell cultures (Fig. 3b, d, f, and h; Fig. 4b, d, and f). Polycaryons appeared 18 h after infection of BFTy cells and 12 h after infection of BFB cells (Table 2). The number of polycaryons increased, but their size remained relatively small. The highest numbers of nuclei per polycaryon were 15 in BFTy cells at 20 h and 22 in BFB cells at 18 h after infection. Fusion between polycaryons did not seem to occur, since they degenerated, lysed, and detached after reaching the size mentioned. Single cells also developed cytopathic changes identical to those in cultures without trypsin.

Polycaryocytosis in trypsin-treated BFTy and BFB cells depended on de novo HA synthesis (Table 2). The HA released into the fluid occurred earlier and was higher by several factors in trypsin-treated, infected cell cultures. Exposure of monolayers to L9 virus of high HA activity and infectivity propagated in the presence or absence of trypsin did not induce fusion from without under our experimental conditions. Also, L9 viral suspensions produced in the presence or absence of trypsin having HA titers ranging from 4 to 4,096 did not hemolyze mouse erythrocytes, an optimal type of erythrocyte with receptors for the L9 HA.

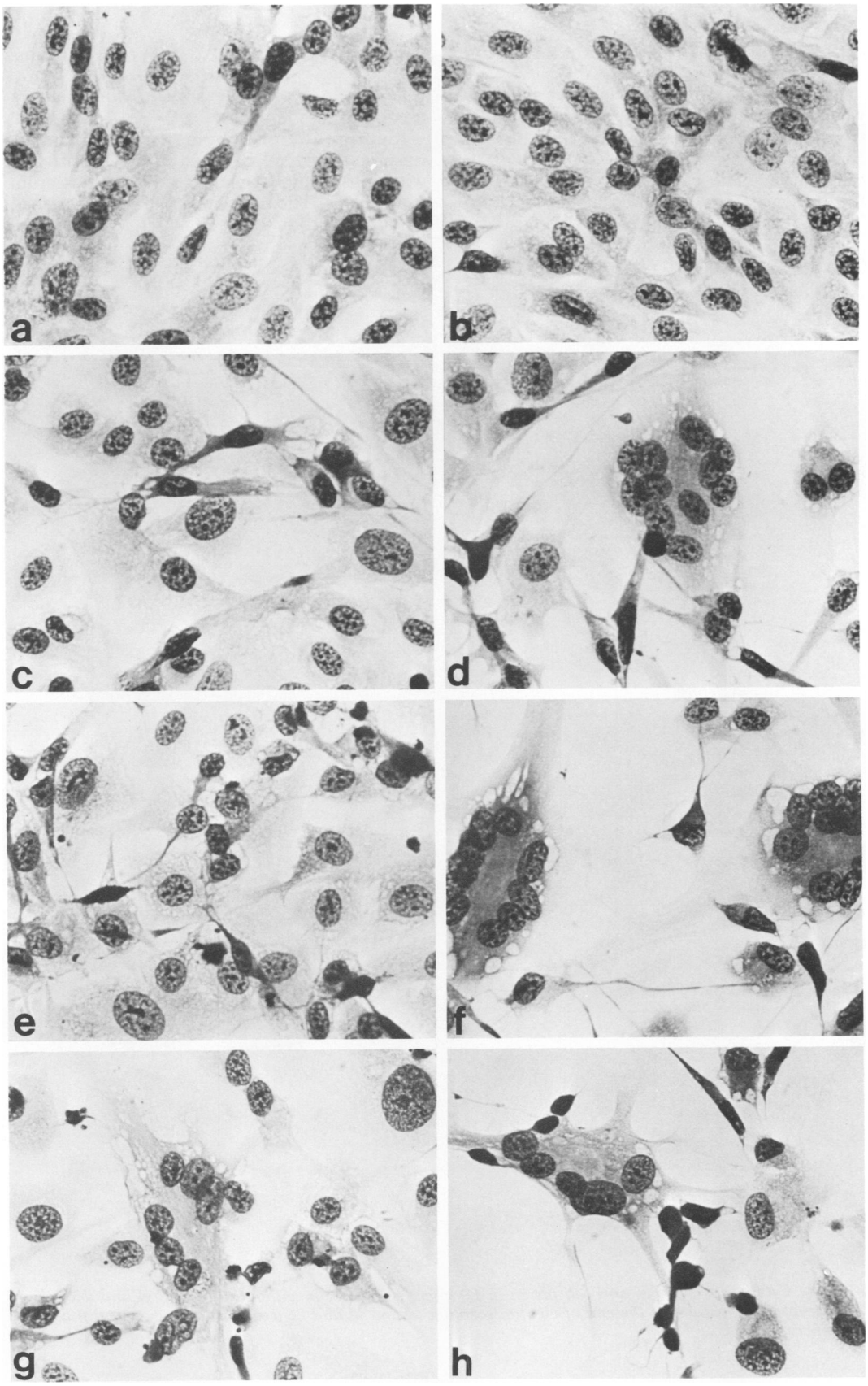

FIG. 3. *Cytopathic changes and cell fusion in L9-infected BFTy cells without (a, c, e, and g) and with (b, d, f, and h) trypsin in the medium at the end of viral adsorption (a and b) and 22 (c and d), 29 (e and f), and 45 (g and h) h later. Magnification, ×400.*

Infectivity yield. The yields of infectivity when L9 virus was propagated with and without trypsin under one-step growth conditions are given in Fig. 5. Infectivity was released from cells earlier. The cell-associated infectivity in the presence of trypsin was higher by 1 $\log_{10}$ than that in trypsin-free cultures, which reflects a 90% increase in yield.

Identity and morphology of L9 virus. Virus propagated in BFTy and BFB cells with and without trypsin was neutralized by L9 antiserum from calves. The morphology of virus obtained

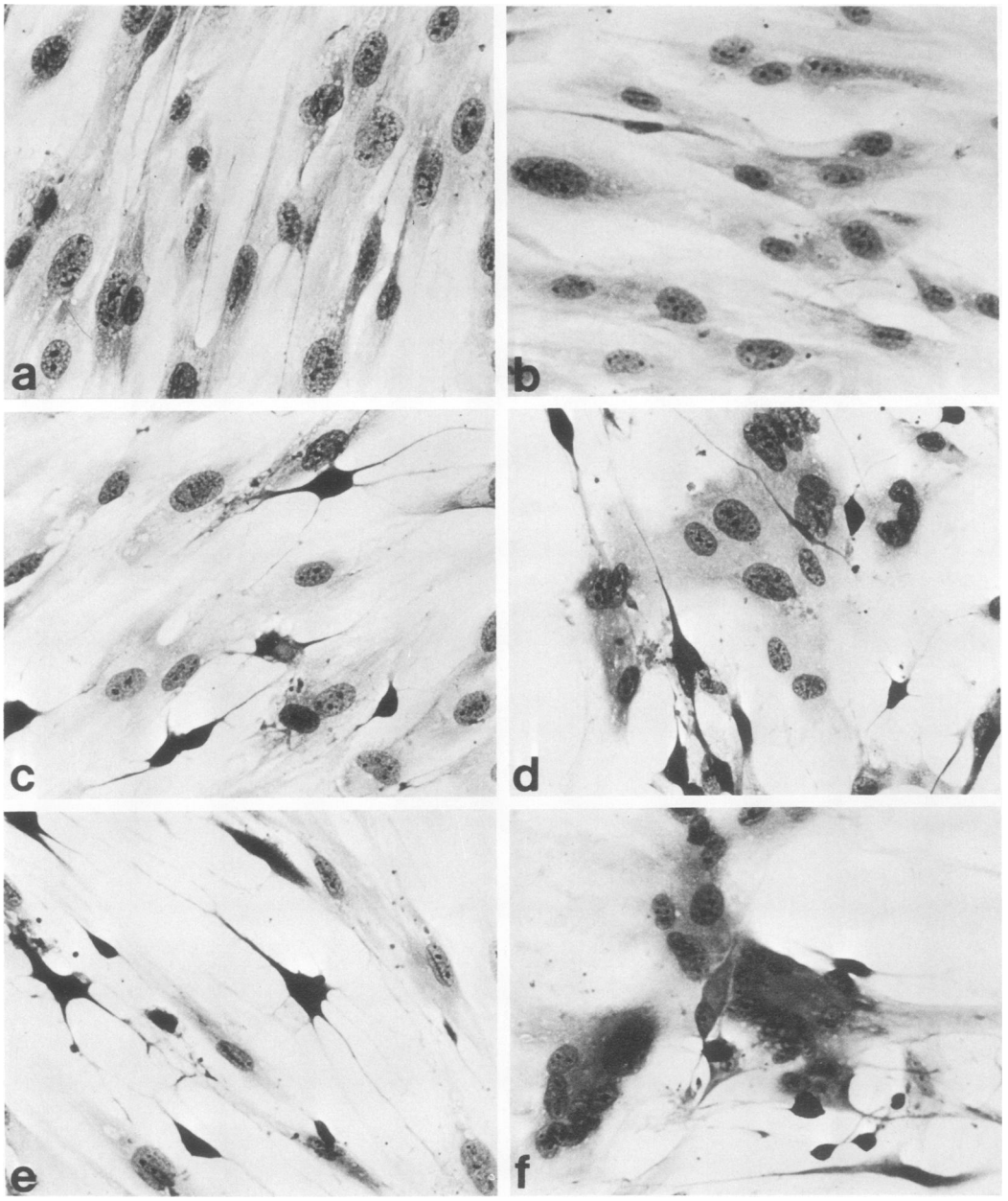

FIG. 4. *Cytopathic changes and cell fusion in L9-infected BFB cells without (a, c, and e) and with (b, d, and f) trypsin in medium at the end of viral adsorption (a and b) and 21 (c and d) and 36 (e and f) h later. Magnification, ×400.*

TABLE 2. *Bovine coronavirus L9 replication in BFTy and BFB cells and the effect of trypsin on cytopathic functions*

Cell type	Hours after inoculation	Cell fusion[a]		Nuclei/polycaryon	Cell-free HA antigen titer	
		No trypsin	Trypsin		No trypsin	Trypsin
BFTy	3	–	–	0	<2	<2
	6	–	–	0	<2	<2
	12	–	–	0	<2	8
	18	–	+	2-5	4	8
	20	–	+	3-15	8	32
	24	–	+	3-12	8	32
	36	–	+	3-12	32	64
	48	+	+	3-12	32	128
BFB	3	–	–	0	<2	<2
	6	–	–	0	<2	<2
	12	–	+	3-4	<2	4
	18	–	+	3-8	<2	32
	20	–	+	5-22	4	32
	24	–	+	5-20	4	64
	36	–	+	8-20	32	256
	48	–	+	8-20	128	512

[a] –, No polycaryons detectable; +, polycaryons present.

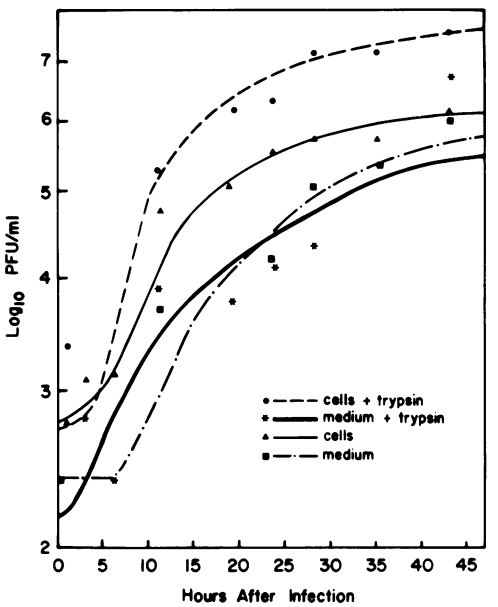

FIG. 5. *One-step growth curve of coronavirus strain L9 in BFTy cells. Cell-released virus in cultures without (—·—) and with (——) trypsin; cell-associated virus without (——) and with (---) trypsin.*

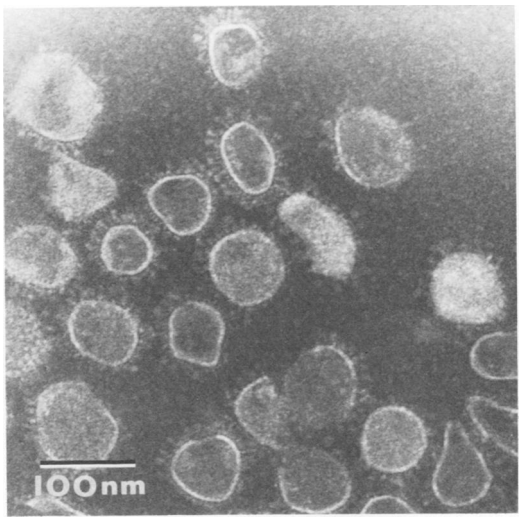

FIG. 6. *Negatively stained viral particles from BFTy cells infected with coronaviral strain L9 without trypsin in the medium. Most particles are flatly collapsed and covered by stain. White, unstained rings marking periphery of envelopes are prominent.*

under these conditions in BFTy cells is shown in Fig. 6, 7, and 8. Three types of coronavirus particles were seen in fluids of trypsin-free cultures: pleomorphic, flat particles penetrated or covered by stain and varied in size from 80 to 120 nm; collapsed particles covered by stain and with a marked unstained ring describing the contours of the round envelope; and particles that excluded the stain completely and varied least in diameter (80 to 100 nm). All of these particles had variably long surface projections (15 to 22 nm). Wedge-shaped enlargements terminated the longer projections (Fig. 6 and 7). The first two types of particles described for trypsin-free cultures were also found in fluids of trypsin-treated, infected cell cultures. These appeared to be immature or defective particles, since their envelopes did not seem to contain

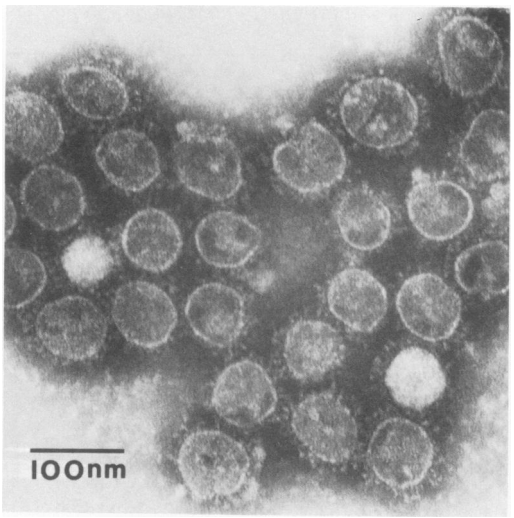

FIG. 7. *Negatively stained viral particles from BFTy cells maintained in trypsin-free medium. Two white particles excluded stain completely. Surface projections on envelope are detectable on all particles.*

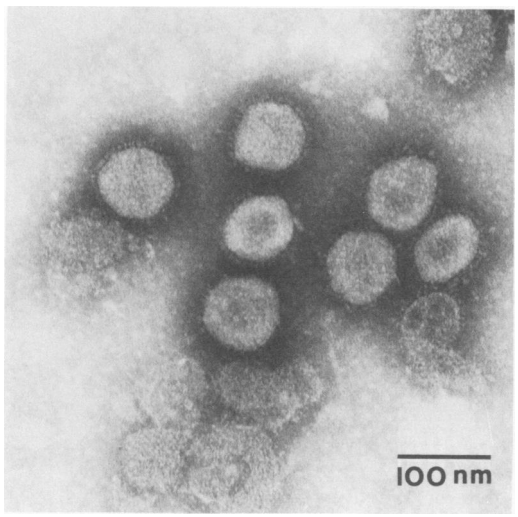

FIG. 8. *Negatively stained viral particles from BFTy cells infected with coronavirus strain L9 and maintained on medium containing 10 μg of trypsin per ml. Virions excluding stain have surface projections half the length of those in Fig. 6 and 7.*

sufficient core substance to prevent flattening and covering by stain. The third form of coronavirus, which excluded stain completely from the envelope confinement, was more numerous in trypsin-treated cultures. The diameter of the virtually round particles ranged between 80 and 90 nm. The spikes, or surface projections, of these particles were more regularly arranged and not longer than 10 nm (Fig. 8). The long surface structures of trypsin-free cultures were not found on these particles. Significantly, our electron microscopic techniques provided relatively pure viral preparations after a 20-min differential centrifugation of fluid from infected cells. The coronaviral particles observed, therefore, must represent cell-released virions unaltered by purification procedures.

DISCUSSION

Plaque development of the enteropathogenic coronavirus strain L9 in BFTy and BFB cells was clearly enhanced by the presence of trypsin in the overlay, so that plaques became uniformly larger and could be read within 3 days of plating, instead of the 6 days after plating required for plaques on medium without trypsin in the overlay. A similar effect of trypsin was described earlier for plaque induction by influenza viruses (1, 18).

This coronavirus strain replicated in BFTy and BFB cells without trypsin, but induced only mild cytopathic changes in the cell monolayers. Release of HA antigen, cell-associated viral infectivity yields, and cytopathic functions were enhanced by trypsin action. Cultivation of enteropathogenic coronaviruses and their isolation from clinical specimens still remains a difficult task. Many coronaviral strains either could not be propagated in cultured cells (5, 7, 12, 21) or could be propagated only in organ cultures (3, 4, 14). Some differentiated cell types cultured from intestinal or other forms of cancer were recently found suitable for improved coronavirus propagation (13, 20, 27, 28). Trypsin treatment accelerated cytopathic functions, facilitated cell fusion, and improved HA as well as infectivity yields in the L9-BFTy and L9-BFB systems, cells derived from normal fetuses. We are now testing the suitability of our systems for isolating additional coronavirus strains from naturally occurring intestinal infections.

A most striking effect of trypsin was the activation of the cell fusion function in the cytopathic expression of this infection in both cell types. Cell fusion in L9-virus-infected cell cultures depended almost absolutely on the presence of trypsin. Only fusion from within related to de novo synthesis of HA antigen and infectivity was observed. The polycaryons reached a maximum size of 15 to 22 nuclei in BFTy and BFB cells, respectively, and then they detached and lysed. Secondary fusion between polycaryons was not observed. The functions of only two of the structural and nonstructural proteins of coronaviruses have been identified (25, 26, 28). Our system might help to clarify the identity of the fusion factor involved in cytopathic expression of coronavirus replication, unless the

trypsin effect influences only cellular reactions.

The findings described here imply that host cell factors, such as the presence of trypsin or other proteolytic enzymes within the host cell or in its environment, play an important role in the expression of cytopathic function of the L9 coronavirus strain. Interestingly, intestinal sites with proteolytic enzyme activity also are most severely affected by this infection (6). This enhancement by trypsin probably functions with other enteropathogenic coronaviruses. The replication of enteropathogenic rotaviruses also is enhanced by trypsin (2). The mechanisms of trypsin enhancement of cytopathic viral functions most likely differ between rotaviruses and coronaviruses. The dependence of cell fusion activity on trypsin in our systems relates the mechanism somehow to the classical observation on proteolytic activation of cell fusion activity in paramyxovirus infections of certain cells (8-11, 17-19). The precursor glycoprotein F_0 is proteolytically cleaved to the smaller F, which assumes cell fusion activity (11, 19). Sturman and Holmes (26) emphasized the requirements of posttranslational viral protein processing in the morphogenesis of the mouse coronavirus strain A59 propagated in 17CL1 cells, a spontaneously transformed BALB/C3T3 cell line, but they did not find significant enhancement of infectivity or other viral functions by trypsin treatment. A 180K glycoprotein was cleaved to 90K molecules (26).

Trypsin-treated BFTy cells generated virus particles that excluded phosphotungstic acid stain from the envelope confinement and had distinctly shorter, more regularly arranged surface projections. These particles differed from stain-covered, flattened, or incomplete particles of both cultural conditions, as well as from the stain-excluding virions of trypsin-free BFTy cultures. The envelope surface projections of all of these other forms were at least twice as long. The virions were gently processed for ultrastructural analysis. The particles impregnated by stain in our studies resembled the forms of coronavirions from avian infectious bronchitis which McNaughton and Davies (15) identified as defective.

ACKNOWLEDGMENTS

These investigations were made possible through an Alexander Humboldt Award to J.S. for a year of research at the Virology Institute of the Justus Liebig University, Giessen, Germany. Support for the investigations also came from the Sonderforschungsbereich 47 (Deutsche Forschungsgemeinshaft), from the Regional Project W-112, and from Special Research grant 02-105, Science and Education Administration, U.S. Department of Agriculture.

We thank Eva Kroell, Deryl Keney, and Mary Hegedus for skillful assistance.

LITERATURE CITED

1. **Appleyard, G., and H. B. Maber.** 1974. Plaque formation by influenza viruses in the presence of trypsin. J. Gen. Virol. **25**:351-357.
2. **Babiuk, L. A., K. Mohammed, L. Spence, M. Fauvel, and R. Petro.** 1977. Rotavirus isolation and cultivation in the presence of trypsin. J. Clin. Microbiol. **6**:610-617.
3. **Bridger, J. C., E. O. Caul, and S. I. Egglestone.** 1978. Replication of an enteric bovine coronavirus in intestinal organ cultures. Arch. Virol. **57**:43-51.
4. **Caul, E. O., and S. K. R. Clarke.** 1975. Coronavirus propagated from patient with nonbacterial gastroenteritis. Lancet **ii**:953-954.
5. **Caul, E. O., W. K. Paner, and S. K. R. Clarke.** 1975. Coronavirus particles in faeces from patients with gastroenteritis. Lancet **i**:1192.
6. **Doughri, A. M., and J. Storz.** 1977. Light and ultrastructural pathologic changes in intestinal coronavirus infection of newborn calves. Zentralbl. Veterinaermed. Reihe B **24**:367-385.
7. **Doughri, A. M., J. Storz, I. Hajer, and H. S. Fernando.** 1976. Morphology and morphogenesis of a coronavirus infecting intestinal epithelial cells of newborn calves. Exp. Mol. Pathol. **25**:355-370.
8. **Holmes, K. V., and P. W. Choppin.** 1966. On the role of the response of the cell membrane in determining virus virulence. Contrasting effects of the parainfluenza virus SV5 in two cell types. J. Exp. Med. **124**:501-520.
9. **Homma, M.** 1971. Trypsin action on the growth of Sendai virus in tissue culture cells. I. Restoration of the infectivity for L cells by direct action of trypsin on L cell-borne Sendai virus. J. Virol. **8**:619-629.
10. **Homma, M.** 1972. Trypsin action on the growth of Sendai virus in tissue culture cells. II. Restoration of the hemolytic activity of L cell-borne Sendai virus by trypsin. J. Virol. **9**:829-835.
11. **Homma, M., and S. Tamagawa.** 1973. Restoration of the fusion activity of L cell-borne Sendai virus by trypsin. J. Gen. Virol. **19**:423-426.
12. **Kapikian, A. Z., H. D. James, S. J. Kelly, and A. L. Vaugh.** 1973. Detection of coronavirus strain 692 by immuno-electron microscopy. Infect. Immun. **7**:111-116.
13. **Laporte, J., R. L'Haridon, and P. Bobulesco.** 1979. In vitro culture of bovine enteritic coronavirus. INSERM Inst. Natl. Sante Rech. Med. Colloq. **90**:99-102.
14. **McIntosh, K.** 1974. Coronaviruses: a comparative review. Curr. Top. Microbiol. Immunol. **63**:85-129.
15. **McNaughton, M. R., and H. A. Davies.** 1980. Two particle types of avian infectious bronchitis. J. Gen. Virol. **47**:365-372.
16. **Mebus, C. A., E. L. Stair, M. B. Rhodes, and M. J. Twiehaus.** 1973. Neonatal calf diarrhea: propagation, attenuation, and characteristics of a coronavirus-like agent. Am. J. Vet. Res. **34**:145-150.
17. **Nagai, Y., H. D. Klenk, and R. Rott.** 1976. Proteolytic cleavage of the viral glycoproteins and its significance for the virulence of Newcastle Disease Virus. Virology **72**:494-508.
18. **Rott, R.** 1979. Molecular basis of infectivity and pathogenicity of myxovirus. Brief review. Arch. Virol. **59**: 285-298.
19. **Scheid, A., and P. W. Choppin.** 1974. Identification of biological activities of paramyxovirus glycoproteins. Activation of cell fusion, hemolysis, and infectivity by proteolytic cleavage of an inactive precursor protein of Sendai virus. Virology **57**:475-490.
20. **Schmidt, O. W., M. K. Cooney, and G. E. Kenny.** 1979. Plaque assay and improved yield of human coronaviruses in a human rhabdomyosarcoma cell line. J. Clin. Microbiol. **9**:722-728.
21. **Schnagl, R. D., I. H. Holmes, and E. M. Mackay-**

Scollay. 1978. Coronavirus-like particles in Aboriginals and non-Aboriginals in Western Australia. Med. J. Aust. **1**:307–310.

22. **Sharpee, R. L., C. A. Mebus, and E. P. Bass.** 1976. Characterization of a calf diarrheal coronavirus. Am. J. Vet. Res. **37**:1031–1041.
23. **Storz, J., N. Okuna, A. E. McChesney, and R. E. Pierson.** 1976. Virologic studies on cattle with naturally occurring and experimentally induced malignant catarrhal fever. Am. J. Vet. Res. **37**:875–878.
24. **Storz, J., and R. Rott.** 1980. Über die Verbreitung der Coronavirusinfektion bei Rindern in ausgwählten Gebieten Deutschlands: Antikörpernachweis durch Mikroimmundiffusion und Neutralisation. Dtsch. Tieraerztl. Wochenschr. **87**:252–254.
25. **Sturman, L. S.** 1977. Characterization of a coronavirus. I. Structural proteins: effects of preparative conditions on the migration of protein in polyacrylamide gels. Virology **77**:637–649.
26. **Sturman, L. S., and K. V. Holmes.** 1977. Characterization of a coronavirus. II. Glycoproteins of the viral envelope: tryptic peptide analysis. Virology **77**:650–660.
27. **Sturman, L. S., and K. K. Takemoto.** 1972. Enhanced growth of a murine coronavirus in transformed mouse cells. Infect. Immun. **6**:501–507.
28. **Wege, H., H. Wege, K. Nagashima, and V. ter Meulen.** 1979. Structural polypeptides of the murine coronavirus JHM. J. Gen. Virol. **42**:37–47.